Available online at www.sciencedirect.com
ScienceDirect
Trans. Nonferrous Met. Soc. China 28(2018) 1602−1610
Transactions of Nonferrous Metals Society of China
www.tnmsc.cn

Fabrication and application of nano/microcrystalline composite diamond coated drawing dies using alternative carbon sources

Cheng-chuan WANG, Xin-chang WANG, Fang-hong SUN

School of Mechanical Engineering, Shanghai Jiao Tong University, Shanghai 200240, China

Received 18 April 2017; accepted 18 September 2017

Abstract: Nano/microcrystalline composite diamond films were deposited on the holes of WC−6%Co drawing dies by a two-step procedure using alternative carbon sources, i.e., methane for the microcrystalline diamond (MCD) layer and acetone for the nanocrystalline diamond (NCD) layer. Moreover, the monolayer methane-MCD and acetone-NCD coated drawing dies were fabricated as comparisons. The adhesion and wear rates of the diamond coated drawing dies were also tested by an inner hole polishing apparatus. Compared with mono-layer diamond coated drawing die, the composite diamond coated one exhibits better comprehensive performance, including higher adhesive strength and better wear resistance than the NCD one, and smoother surface (R_a=65.3 nm) than the MCD one (R_a=95.6 nm) after polishing at the same time. Compared with the NCD coated drawing die, the working lifetime of the composite diamond coated one is increased by nearly 20 times.

Key words: microcrystalline; nanocrystalline; composite diamond film; WC−Co drawing die; alternative carbon source

1 Introduction

Drawing dies are important tools to produce wires, cables or tubes with various sizes in wire and cable drawing industries. However, uncoated WC−Co drawing dies can be worn easily, which will decrease the working lifetime of dies and cannot ensure the dimensional precision and smoothness of as-drawn metal wires. As a result, depositing uniform chemical vapor deposition (CVD) diamond film is an effective way to improve the wear resistance of drawing dies [1].

Due to the excellent characteristics such as high mechanical hardness, large thermal conductivity, great wear resistance and corrosion resistance, CVD diamond films have received considerable attentions in many fields [2]. Hot filament CVD (HFCVD) is the most commonly-used way for depositing diamond films. This technique has many advantages, such as simple operation, low cost and good security [3]. WEI et al [4,5] synthesized diamond films with different micro morphologies using methane source by adjusting deposition parameters. MAN et al [6] deposited diamond films when the carbon source is composed of CH_3OH−H_2 gas mixture through microwave plasma enhanced CVD. Based on the acetone−hydrogen system, nanocrystalline diamond (NCD) films were deposited on silicon wafers by decreasing the gas pressure and increasing the concentration of hydrocarbon with HFCVD technique by WANG et al [7]. In addition, acetylene, diethylether and trimethylamine have also been chosen as carbon sources to obtain diamond films in different atmospheres [8].

There are also many studies focused on CVD diamond film growth on interior holes of drawing dies for optimizing diamond deposition parameters [9,10] or investigating the wear and tribological performance of diamond-coated dies [11,12]. Nonetheless, due to the columnar structure and rough surface topography, conventional microcrystalline diamond (MCD) films are quite difficult to be polished to ensure the required smoothness. Besides, the polishing process of MCD films will consume too much time and seriously decrease the efficiency of the mass production of diamond coated drawing dies [13]. Therefore, it is necessary to deposit a layer of diamond film that could be polished easily to provide high surface finish for the inner holes of drawing dies.

Nowadays, the commonly-used carbon sources to deposit CVD diamond films on WC−Co drawing dies are

Foundation item: Project (51275302) supported by the National Natural Science Foundation of China
Corresponding author: Fang-hong SUN; Tel: +86-21-34206557; E-mail: sunfanghong@sjtu.edu.cn
DOI: 10.1016/S1003-6326(18)64802-2

methane [10,14] and acetone [1,13]. CHANDRAN et al [14] obtained NCD-coated die, decreasing the residual stress of as-produced tubes, reducing tube roughness and lowering the temperature rise caused by the deformation in the drawing process, but the working lifetime of dies cannot be improved. SUN et al [13] developed a new technology to deposit nano/microcrystalline composite diamond films on the hole surfaces of WC−Co cemented carbide substrates, with which the quality and smoothness of as-drawn products have been improved. However, only the acetone was used as the carbon source in this research, so it could be speculated that there are still some rooms for improvement on the performance and working lifetime of diamond coated dies if various carbon sources are applied. According to previous study, it can be concluded that the methane-MCD film showed better adhesion than the acetone-MCD film [15]. Furthermore, WANG et al [16] also mentioned that methane-MCD film is more difficult to be worn than acetone-MCD film, which means that the diamond films synthesized using the acetone could be polished easier than those synthesized using methane.

In the present work, a special bilayer MCD/NCD composite diamond film synthesized using two alternative carbon sources (methane and acetone) is designed and deposited on the inner hole surface of the drawing die. The FESEM (Zeiss ULTRA55), surface roughness, Raman spectroscopy (SPEC14-03) and XRD (D8 ADVANCE) are employed for characterizing the composite diamond film, as well as monolayer methane-MCD and acetone-NCD films that are adopted as comparisons. Moreover, the adhesion and wear rate testing and actual application of the diamond-coated drawing dies are also conducted.

2 Experimental

The WC−Co drawing dies (d22 mm × 18 mm) with aperture of d5.23 mm were used as substrates. A two-step pretreatment was employed on all these substrates to roughen the hole surfaces and remove the Co binder phase from the substrates: ultrasonic agitation in the Murakami's reagent (10 g $K_3[Fe(CN)_6]$ +10 g KOH + 100 mL H_2O) for 30 min and cobalt etching in the Caro's acid (20 mL HCl + 80 mL H_2O_2) for 30 s. Afterwards, the drawing dies were abraded with hard cloth attached to diamond suspension (0.5 μm) on a home-made rotational equipment and then cleaned in an ultrasonic bath dipping in acetone. A home-made HFCVD apparatus was used during the deposition process, and a DC biasing was exerted on the substrate holder for enhancing the diamond nucleation (positive biasing) [17,18] and refining the crystals of the diamond (negative biasing) [3,19].

The drawing die was located by the copper fixture, and the hot filaments (d0.6 mm) made of two dragged tantalum wires passed through the center of the die. The filament temperature was measured by an infrared thermometer and the substrate temperature was measured using a Type K thermocouple attached to the entry zone of dies, kept at around 830 °C. Methane and acetone were applied as the carbon sources in the deposition. Methane and hydrogen could be directly introduced into the chamber, while the liquid carbon source acetone had to be taken into the reactor by bubbling part of H_2 through the liquid. The pressure of acetone was associated with its temperature, so the liquid carbon source was kept at 0 °C by immersing the acetone container in glacial-aqueous mixed solution [20]. The detailed deposition parameters for two kinds of diamond films are listed in Table 1. In addition, the composite diamond films were synthesized using methane and hydrogen for 3 h firstly (MCD-1), and then by adjusting parameters without interruption, the second layer nanocrystalline diamond films (NCD-2) were deposited on the first layer using acetone and hydrogen for another 3 h.

The diamond coated drawing dies needed to be polished before their actual application because of the production of surface precision demand. Therefore, the interior-hole polishing machine transformed by manual lathe was adopted to polish inner hole surfaces of the as-deposited drawing dies with diamond grits (10 μm). Afterwards, the diamond-coated drawing die samples were cut into four parts equally along their axis direction by wire-electrode cutting. The FESEM was applied to observe the surfaces and cross-sectional morphologies of the diamond films. The Raman spectroscopy and XRD were employed to analyze the ingredients and purity of the films. In addition, a home-designed abrasive wear tester was used to evaluate the adhesion of the as-fabricated films and study their wear resistance. In the test, a low-carbon steel wire with a size specification of about d5.3 mm was plugged into the hole of the die with

Table 1 Deposition parameters for two kinds of diamond films

Carbon source	Carbon source content/%	Total pressure/ 133.322 Pa	Filament temperature/°C	Substrate temperature/°C	Bias current/A	Duration/min
Methane (MCD-1)	4.7	15−36	2000±10	830±20	2	360
Acetone (NCD-2)	2.2−3.2	9.8−38	2000±10	830±20	2/−0.1	360

an interference fit. Then, the die rotated at a rotational velocity of 300 r/min while the wire reciprocated along the axial direction at a linear velocity of 0.3 m/s. During the process, diamond powders (5 μm) mixed with lubricating oil were added into the inner holes periodically. The diameter reduction of the die holes were measured every 3 min for evaluating the wear rates and observing the peeling-off phenomenon of the films.

3 Results and discussion

3.1 Characterization of diamond coated drawing dies

In order to get the surface and cross-sectional morphologies of the diamond films deposited on the inner holes of drawing dies before and after polishing, these drawing dies were cut into four parts on average. Then, one quarter of each die was observed by scanning electron microscope at three different positions (A_1−entry zone, A_2−compression zone, A_3−bearing zone). The surface morphologies before and after polishing are shown in Fig. 1 and Fig. 2, respectively. The cross-sectional morphologies are also presented in Fig. 1. As illustrated in Figs. 1(a−c), the die holes are covered by microcrystalline diamond film, which is fabricated using methane and predominate in (100) facet. The average size of its crystal is about 3 μm. Figures 1(d−i) present nanocrystalline diamond films which are cauliflower-structured. The morphologies after polishing are shown in Fig. 2, in which we can observe that the bearing zones of all films are the smoothest ones. However, the MCD surface appears rougher than that of the other two diamond films because of the presence of its obvious grooves. Additionally, the specific film thickness values are presented in Table 2. The coating gets thicker from A_1 zone to A_3 zone in the same die. The different growth rates are caused by the different temperature distributions because the distances between the filament and the hole surface at three zones are different. Among these diamond films, the thickness difference of the MCD film at different zones is the largest, and the monolayer NCD film has the most uniform thickness distribution. Besides, the growth rates of diamond films corresponding to these thickness values are given in Table 3. The growth rate of the MCD is larger than that of other two films at the same zone while the NCD has the slowest growth rate.

To identify the dual-layer structure of the as-deposited composite diamond film, its cross-sectional morphology enlarged can be seen in Fig. 3. The lower layer of the MCD film is made up of columnar structure with coarse crystals. Differently, the upper NCD layer looks like a stacked structure with some fine sand. It can also be seen that the MCD layer is thicker than the NCD layer despite the same deposition time of the two layers.

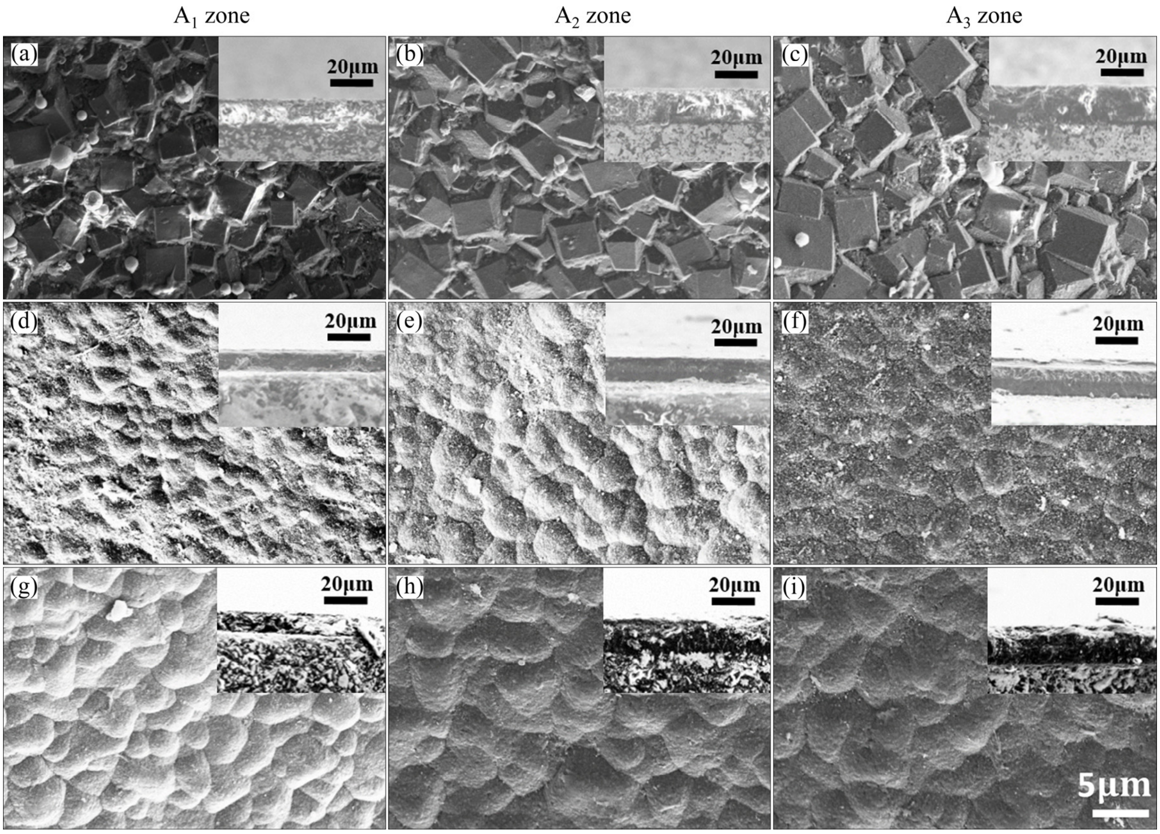

Fig. 1 Surface and cross-sectional morphologies of three kinds of diamond films on drawing dies: (a−c) MCD films; (d−f) NCD films; (g−i) Composite diamond films

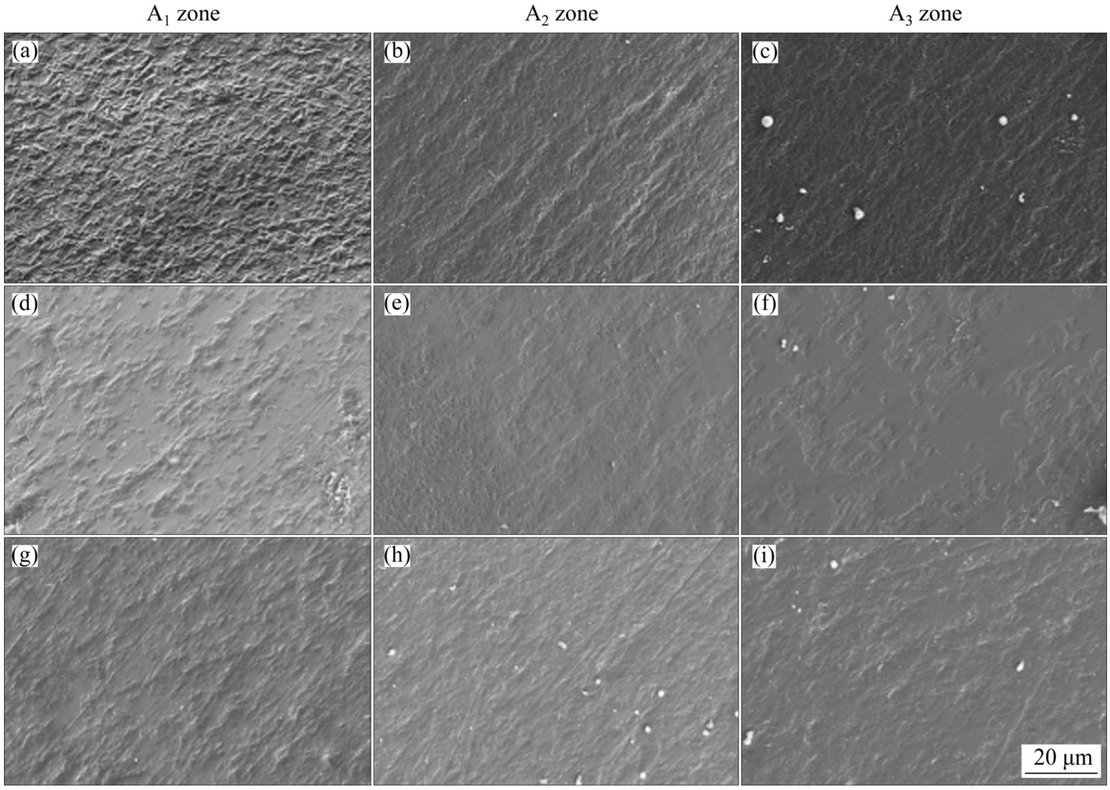

Fig. 2 Surface morphologies of three kinds of diamond films after polishing on drawing dies: (a−c) MCD films; (d−f) NCD films; (g−i) Composite diamond films

Table 2 Film thickness at different zones of drawing die

Type	Film thickness/μm		
	A_1 zone	A_2 zone	A_3 zone
MCD film	11.62	16.62	17.96
NCD film	9.25	12.18	14.63
Composite diamond film	9.62	16.42	16.75

Table 3 Film growth rate at different zones of drawing die

Type	Film growth rate/(μm·h^{-1})		
	A_1 zone	A_2 zone	A_3 zone
MCD film	1.94	2.77	2.99
NCD film	1.54	2.03	2.44
Composite diamond film	1.60	0.73	2.79

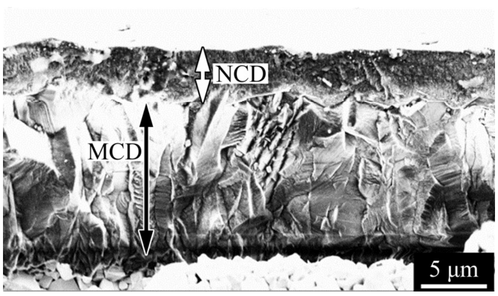

Fig. 3 Enlarged cross-sectional morphology of composite diamond films at A_3 zone

This is due to the use of negative biasing for 1 h during the NCD deposition, which mainly has an effect on refining diamond crystal. However, during this process, the diamond deposition rate maybe decreases, which makes the NCD layer show different growing rates compared with the monolayer MCD film.

Before being applied on the production line, the diamond coated drawing dies need to be polished for meeting production requirements. A simple lathe was modified as a polishing equipment to trim inner hole surfaces of these drawing dies. Considering the main working load that the bearing zone of the drawing die bears, the surface roughness R_a on the zone, measured with 4 mm scanning length using PGI 420 profiler (Taylor Hobson) before and after polishing is shown in Table 4. The polishing time is also indicated in Table 4, among which the roughness of the MCD coated die cannot be further improved even with more polishing

Table 4 Surface roughness R_a of diamond films at A_3 zone on drawing die before and after polishing

Type	Polishing time/h	R_a/nm	
		Before polishing	After polishing
MCD film	1	322.6	95.6
NCD film	0.5	91.8	67.6
Composite diamond film	0.5	243.7	65.3

time. From the comparable results, it can be concluded that before polishing, the NCD film has the smoothest surface because of its nanomorphology. On the contrary, the composite diamond film shows a greater R_a under the effects of the coarse MCD layer. However, after polishing, the composite diamond film reaches the same roughness level as the NCD film, which can also be gotten by observing the morphologies in Fig. 2.

Raman spectroscopy is a very effective way to characterize the structure of diamond films including the bonding type, film homogeneity etc at three different zones of drawing die. The Raman spectra of the as-deposited diamond films shown in Fig. 4, using an Ar^+ laser with an excitation wavelength of 532 nm, were deconvoluted and analyzed by G−L (Gauss−Lorentz) peak fitting with linear background subtraction [21].

As shown in Fig. 4, there are some differences in different zones of the same die because of the complex geometry of drawing die, which results in the non-uniform fabricated films. For the MCD film, the Raman spectra (Figs. 4(a−c)) exhibit sharp peaks near 1332 cm^{-1} with FWHM of ~13.02 cm^{-1}, which indicates its high purity at three zones. Figures 4(a) and (b) show a distinct crystalline component at approximately 1350 cm^{-1} attributed to amorphous carbon. Nevertheless, it would not cause distinct effects on diamond crystallinity. In comparison, the Raman spectra of the monolayer NCD film and the composite diamond film are very similar, both showing a broad peak with low intensity at about 1334−1338 cm^{-1} because of many boundaries between diamond grains and the amorphous carbon formed in the boundaries [22]. The broadening of the diamond band

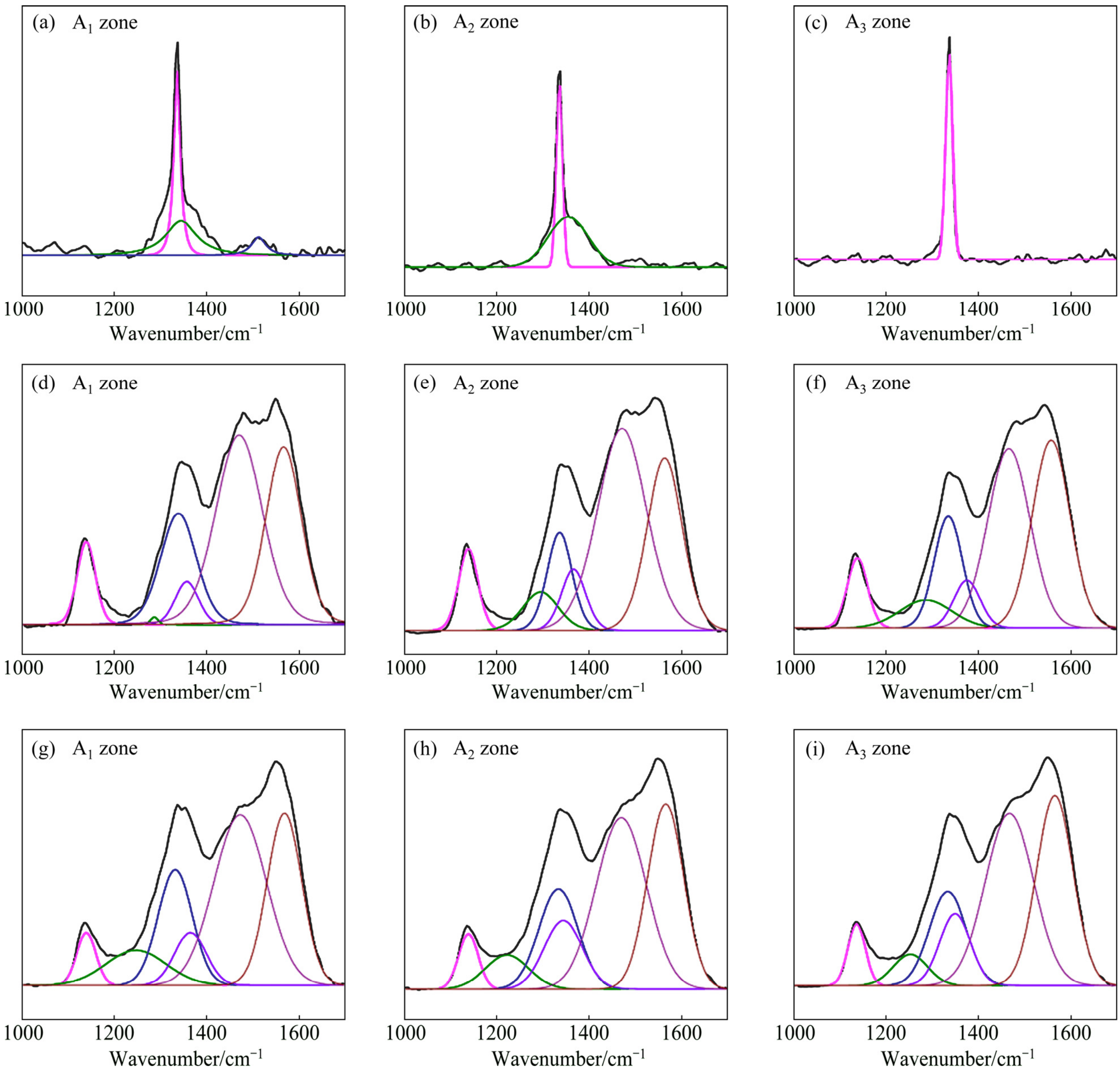

Fig. 4 Raman spectra of three kinds of diamond films on drawing dies: (a−c) MCD film; (d−f) NCD film; (g−i) Composite diamond film

is caused by decreasing the grain size to the nanometer scale, resulting in the decreasing of diamond purity. Besides the diamond peaks, several other typical lines are also visible. The typical broad D-mode (nearly 1350 cm^{-1}) and G-mode (nearly 1560 cm^{-1}) of amorphous carbon are shown in these spectra (Figs. 4(d−i)). In spite of the stronger intensity of non-diamond band, the concentration of diamond still accounts for majority with the fact that the cross-section of Raman scattering is 50−60 times higher for sp^2-bonded carbon [23]. Additionally, the features at 1140 and 1480 cm^{-1} are often used as transpolyacetylene (TPA) segments at the grain boundaries of NCD surface, because they very much resemble the behavior of the ω_1 (in-plane C—H bending combined with C—C stretching) and the ω_3 (C—C stretching) vibration modes of transpolyacetylene [21,24−27]. Previously, a small structure can be distinguished at 1240 cm^{-1} correlated to the maximum in the density of states of phones in diamond [28].

Figure 5(a) shows the image detected by light microscope when taking Raman test. Two testing regions are selected based on the thickness of two layers. Figure 5(b) presents the Raman spectra corresponding to NCD and MCD regions. High intensity and sharp diamond peak is observed on MCD-Raman curve. Both of the MCD and NCD have similar Raman spectra with those of the monolayer ones shown in Fig. 5. Obviously, this result demonstrates that the composite diamond film has two-layer structure.

The crystalline structure of the as-deposited diamond films was detected by XRD with Cu K_α (40 kV/40 mA) radiation source. In Fig. 5, the XRD patterns of three samples at their bearing zones are shown. Each spectrum presents diffraction peaks with 2θ values of about 44°, 75.4° and 91.5° corresponding to (111), (220) and (311) reflections of the diamond films, respectively. In addition, it can be seen that (400)

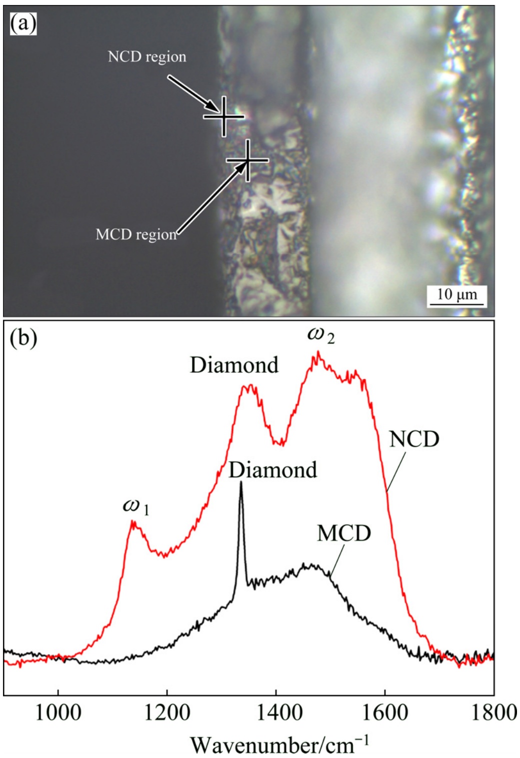

Fig. 5 Cross-sectional details of composite diamond: (a) Microscope image for Raman test; (b) Raman spectra corresponding to NCD and MCD regions, respectively

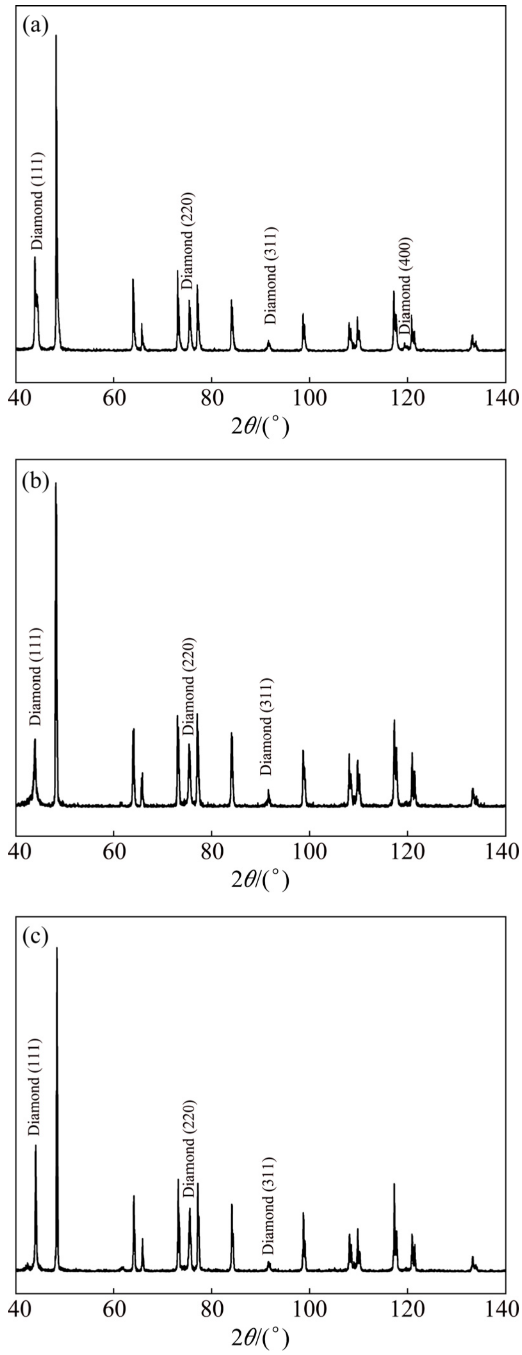

Fig. 6 XRD patterns of three kinds of diamond films at A_3 zone on drawing dies: (a) MCD film; (b) NCD film; (c) Composite diamond film

reflection of MCD at 2θ of 119.5°, whose intensity to that of (111), $I_{(400)}/I_{(111)}$, calculated equals 0.11 according to Fig. 5, stronger than that of randomly oriented diamond power (0.08). Therefore, it can be further confirmed that the cubic facets shown in Fig. 1(c) are (100) crystal faces. Furthermore, the sharp and intense peak in (111) crystal plane confirms the film crystallinity.

3.2 Adhesion and wear rate testing of diamond films

To simulate the real working condition, the diamond coated drawing dies after polishing were employed for adhesion and wear rate testing. Different from diamond films coated on commonly-used plane, conventional indentation or scratch test cannot be used as effective methods to evaluate the coating−die adhesion. Therefore, the film peeling-off time from the drawing die substrate during the wear rate testing is defined as the criterion of adhesion. The wearing rate testing lasts for 36 min for each sample unless the film peels off from the substrate. Then, the results about adhesion and wear resistance are obtained. In the procedure, no peeling is observed on the MCD and composite diamond film while some peelings appear at 18 min on the NCD film. This result is correspondent to the conclusion that films fabricated using methane as carbon source perform better adhesion than that using acetone source [15]. In addition, it has been illustrated that thicker films have lower wear rates [29−31]. Therefore, it may be speculated that the composite diamond film and the MCD film have different wear rates during the test because of their various MCD layer thicknesses.

The wear rates of the as-deposited diamond films were evaluated by the inner hole diameter reduction of the drawing dies. As depicted in Fig. 7, the MCD film, NCD film and composite diamond film exhibit distinct aperture radius variation δ (the measuring accuracy is 0.01 mm) which is the difference between two successive measurements. Among them, the NCD film only lasts for 18 min before the film delamination. The wear rates of the MCD film are a little larger than those of the composite diamond film at the very beginning. This behavior may be caused by the angular (100) plane of the MCD film with the substrate. Afterwards, the MCD film displays better wear resistance than the composite diamond film, which can be attributed to the higher hardness of the MCD film after the smoothing process in the first few minutes. Both of the MCD film and the composite diamond film exhibit a steady wear stage during the normal wearing periods. In 18 min, huge wear appears on the NCD coated drawing die because of the accelerating wear of the exposed WC substrate without coating protection after the delamination of the film.

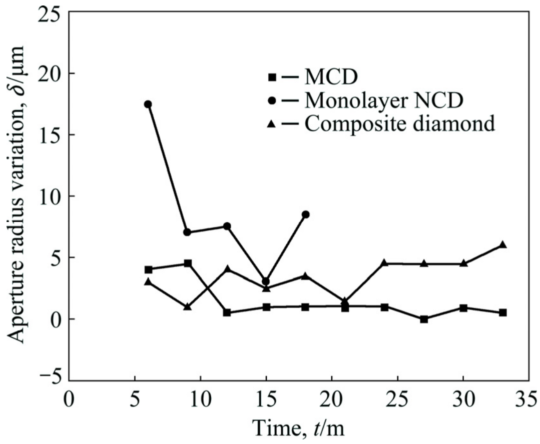

Fig. 7 Aperture radius variations of three kinds of diamond films by wear tests

3.3 Application of diamond coated drawing dies

After the comparison of three different kinds of diamond coated drawing dies, the actual production application was conducted in the industry for drawing low carbon steel wires to investigate their performances. According to the result, the composite diamond coated drawing die shows excellent wear resistance, prolongs working lifetime of the drawing die, increases efficiency of production, and improves the surface smoothness and dimensional precision of the as-produced wires. During the continual usage in the production, about 100 t of low carbon steel wires can be produced with the monolayer NCD coated drawing die, while above 2000 t of low carbon steel wires can be produced with the composite diamond coated drawing dies. However, the low carbon steel wires with some scratches produced by the MCD coated drawing die cannot attain the required surface roughness, which can be concluded from Fig. 8. The roughness (R_a) of wire drawn with composite diamond coated drawing die is 0.19 μm while that is 0.48 μm with MCD coated drawing die. Additionally, unlike the uncoated WC−Co drawing die which must be modified during the interval of wire production, the composite diamond coated drawing die can maintain the production continuity, which can improve the production efficiency by approximately 20%.

4 Conclusions

1) A special type of nano-microcrystalline composite diamond film is coated on cemented tungsten carbide drawing die in a bias-enhanced HFCVD apparatus using alternative carbon sources. Dual-layer structure consists of microcrystalline diamond coated by methane and nanocrystalline film coated by acetone. The cross sectional morphology and Raman spectra both show that the nano-microcrystalline diamond film has a dual-layer structure.

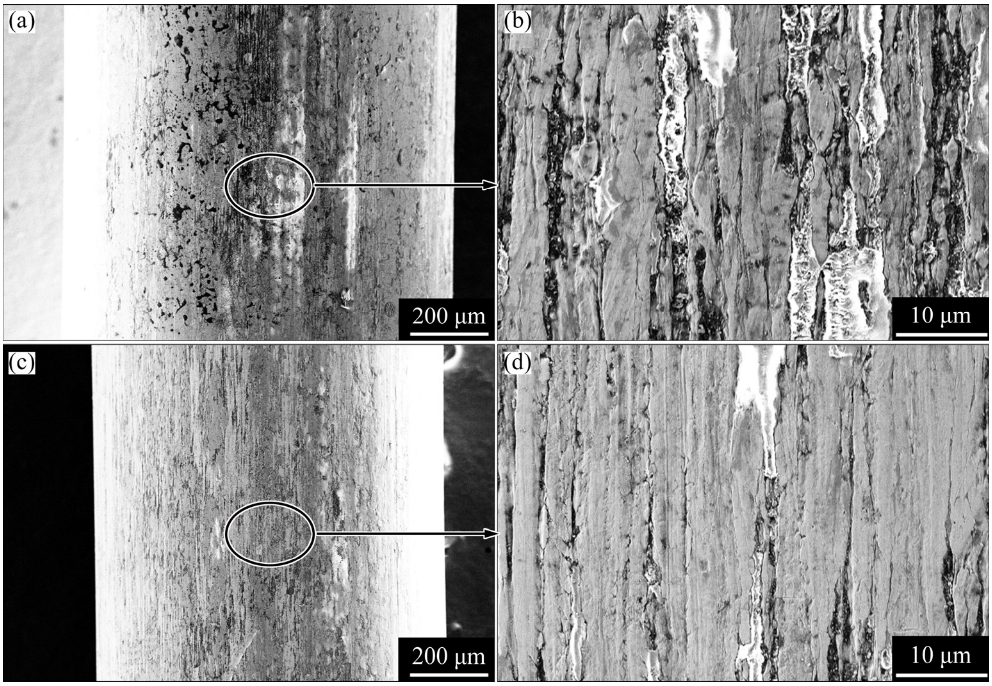

Fig. 8 Images of low carbon steel wires drawn by MCD coated die (a, b) and composite diamond coated die (c, d)

2) The adhesion and wear rate tests show that the adhesive strength and wearing resistance of the composite diamond coated die are both greatly improved compared with the monolayer-coated ones.

3) During the application of drawing dies, the working lifetime of the composite diamond coated drawing dies improves by about 20 times compared with the NCD coated drawing dies. Additionally, the composite diamond film also has a better polishing performance than the monolayer diamond film. The quality of drawn production wires could be guaranteed.

References

[1] ZHANG Zhi-ming, SHEN He-sheng, SUN Fang-hong, HE Xian-chang, WAN Yong-zhong. Fabrication and application of chemical vapor deposition diamond-coated drawing dies [J]. Diamond and Related Materials, 2001, 10: 33−38.

[2] CUI Yu-xiao, ZHANG Jian-guo, SUN Fang-hong, ZHANG Zhi-ming. Si-doped diamond films prepared by chemical vapour deposition [J]. Transactions of Nonferrous Metals Society of China, 2013, 23: 2962−2970.

[3] CHATTOPADHYAY A, SARANGI S K, CHATTOPADHYAY A K. Effect of negative dc substrate bias on morphology and adhesion of diamond coating synthesised on carbide turning tools by modified HFCVD method [J]. Applied Surface Science, 2008, 255: 1661−1671.

[4] WEI Qiu-ping, YU Zhi-ming, ASHFOLD M N R, YE J, MA Li. Synthesis of micro- or nano-crystalline diamond films on WC-Co substrates with various pretreatments by hot filament chemical vapor deposition [J]. Applied Surface Science, 2010, 256: 4357−4364.

[5] WEI Qiu-ping, ASHFOLD M N R, MANKELEVICH Y A, YU Zhi-ming, LIU Pei-zhi, MA Li. Diamond growth on WC−Co substrates by hot filament chemical vapor deposition: Effect of filament−substrate separation [J]. Diamond and Related Materials, 2011, 20: 641−650.

[6] MAN Wei-dong, WANG Jian-hua, LI Lei, ZHANG Bao-hua, BAI Yu-ming. Optical characterization of diamond synthesis using CH_3OH-H_2 gas mixtures [J]. Plasma Science and Technology, 2005, 7: 2748.

[7] WANG Tao, XIN Hai-wei, ZHANG Zhi-ming, DAI Yong-bing, SHEN He-sheng. The fabrication of nanocrystalline diamond films using hot filament CVD [J]. Diamond and Related Materials, 2004, 13: 6−13.

[8] HIROSE Y, TERASAWA Y. Synthesis of diamond thin films by thermal CVD using organic compounds [J]. Japanese Journal of Applied Physics, 1986, 25: L519.

[9] LIN Zi-chao, SUN Fang-hong, ZHANG Zhi-ming, SHEN He-sheng, GUO Song-shou. Optimization of parameters of diamond-coated dies for Cu wire drawing by fem simulations [J]. Advanced Materials Research, 2010, 154−155: 588−592.

[10] WANG Xin-chang, LIN Zi-chao, SHEN Bin, SUN Fang-hong. Effects of deposition parameters on HFCVD diamond films growth on inner hole surfaces of WC−Co substrates [J]. Transactions of Nonferrous Metals Society of China, 2015, 25: 791−802.

[11] LIN Zi-chao, SUN Fang-hong, SHEN Bin. Wear behavior of diamond-coated drawing dies [J]. Transactions of Tianjin University, 2011, 17: 259−263.

[12] NILSSON M, OLSSON M. Tribological testing of some potential PVD and CVD coatings for steel wire drawing dies [J]. Wear, 2011, 273: 55−59.

[13] SUN Fang-hong, MA Yu-ping, SHEN Bin, ZHANG Zhi-ming, CHEN Ming. Fabrication and application of nano–microcrystalline composite diamond films on the interior hole surfaces of Co cemented tungsten carbide substrates [J]. Diamond and Related Materials, 2009, 18: 276−282.

[14] CHANDRAN M, KUMARAN C R, DUMPALA R, SHANMUGAM P, NATARAJAN R, BHATTACHARYA S S, RAMACHANDRA RAO M S. Nanocrystalline diamond coatings on the interior of WC−Co dies for drawing carbon steel tubes: Enhancement of tube

properties [J]. Diamond and Related Materials, 2014, 50: 33−37.

[15] WANG Xin-chang, SHEN Xiao-tian, SUN Fang-hong, SHEN Bin. Mechanical properties and solid particle erosion of MCD films synthesized using different carbon sources by BE-HFCVD [J]. International Journal of Refractory Metals and Hard Materials, 2016, 54: 370−377.

[16] WANG Xin-chang, SHEN Xiao-tian, SUN Fang-hong, SHEN Bin. Tribological properties of MCD films synthesized using different carbon sources when sliding against stainless steel [J]. Tribology Letters, 2016, 61: 1−16.

[17] SAITO D, ISSHIKI H, KIMURA T. Positive-bias enhanced growth of high quality diamond films by microwave plasma chemical vapor deposition [J]. Diamond and Related Materials, 2009, 18: 56−60.

[18] POPOVICI G, CHAO C H, PRELAS M A, CHARLSON E J, MEESE J M. Smooth diamond films grown by hot filament chemical vapor deposition on positively biased silicon substrates [J]. Journal of Materials Research, 2011, 10: 2011−2016.

[19] SEIN H, AHMED W, JACKSON M, POLINI R, HASSAN I, AMAR M, REGO C. Enhancing nucleation density and adhesion of polycrystalline diamond films deposited by HFCVD using surface treatments on Co cemented tungsten carbide [J]. Diamond and Related Materials, 2004, 13: 610−615.

[20] WANG Liang, LEI Xue-lin, SHEN Bin, SUN Fang-hong, ZHANG Zhi-ming. Tribological properties and cutting performance of boron and silicon doped diamond films on Co-cemented tungsten carbide inserts [J]. Diamond and Related Materials, 2013, 33: 54−62.

[21] KLAUSER F, STEINMÜLLER-NETHL D, KAINDL R, BERTEL E, MEMMEL N. Raman studies of nano- and ultra-nanocrystalline diamond films grown by hot-filament CVD [J]. Chemical Vapor Deposition, 2010, 16: 127−135.

[22] CHEN Ming, MA Yu-ping, XIANG Dao-hui, SUN Fang-hong. Study on comparative experiments of performance of conventional and nanocrystalline diamond film [M]. Key Engineering Materials: Trans Tech Publ, 2006: 847−851.

[23] WANG Xin-chang, ZHANG Jian-guo, SHEN Bin, ZHANG Tao, SUN Fang-hong. Fracture and solid particle erosion of micro-crystalline, nano-crystalline and boron-doped diamond films [J]. International Journal of Refractory Metals and Hard Materials, 2014, 45: 31−40.

[24] AZEVEDO A F, MATSUSHIMA J T, VICENTIN F C, BALDAN M R, FERREIRA N G. Surface characterization of NCD films as a function of sp2/sp3 carbon and oxygen content [J]. Applied Surface Science, 2009, 255: 6565−6570.

[25] ABREU C S, AMARAL M, FERNANDES A J S, OLIVEIRA F J, SILVA R F, GOMES J R. Friction and wear performance of HFCVD nanocrystalline diamond coated silicon nitride ceramics [J]. Diamond and Related Materials, 2006, 15: 739−744.

[26] KUZMANY H, PFEIFFER R, SALK N, GÜNTHER B. The mystery of the 1140 cm^{-1} Raman line in nanocrystalline diamond films [J]. Carbon, 2004, 42: 911−917.

[27] NISTOR L C, van LANDUYT J, RALCHENKO V G, OBRAZTSOVA E D, SMOLIN A A. Nanocrystalline diamond films: Transmission electron microscopy and Raman spectroscopy characterization [J]. Diamond and Related Materials, 1997, 6: 159−168.

[28] LOPEZ-RIOS T, SANDRE E, LECLERCQ S, SAUVAIN E. Polyacetylene in diamond films evidenced by surface enhanced Raman scattering [J]. Physical Review Letters, 1996, 76: 4935−4938.

[29] QIN F, CHOU Y K, NOLEN D, THOMPSON R G. Coating thickness effects on diamond coated cutting tools [J]. Surface and Coatings Technology, 2009, 204: 1056−1060.

[30] WEI Qiu-ping, YU Zhi-ming, ASHFOLD M N R, CHEN Zhong, WANG Ling, MA Li. Effects of thickness and cycle parameters on fretting wear behavior of CVD diamond coatings on steel substrates [J]. Surface and Coatings Technology, 2010, 205: 158−167.

[31] LU Ping, GOMEZ H, XIAO Xing-cheng, LUKITSCH M, DURHAM D, SACHDEVE A, KUMAR A, CHOU K. Coating thickness and interlayer effects on CVD-diamond film adhesion to cobalt-cemented tungsten carbides [J]. Surface and Coatings Technology, 2013, 215: 272−279.

基于交替碳源的微纳复合金刚石涂层拉拔模的制备及应用

王成川，王新昶，孙方宏

上海交通大学 机械与动力工程学院，上海 200240

摘　要：基于交替碳源、采用两步法将微纳复合金刚石薄膜沉积在 WC−6%Co 硬质合金拉拔模的内孔基体上，其中甲烷和丙酮分别用于微米层和纳米层的沉积。此外，基于甲烷制备的单层微米金刚石和基于丙酮制备的单层纳米金刚石涂层模具分别作为对照组。金刚石涂层拉拔模具的附着力和磨损率采用内孔抛光设备进行检测。与单层金刚石涂层拉拔模具相比，复合金刚石涂层模具表现出更优异的综合性能，包括比单层纳米金刚石涂层模具更高的附着力和耐磨性，以及在相同时间抛光后比单层微米金刚石涂层(R_a=95.6 nm)模具更光滑的表面(R_a=65.3 nm)。与纳米涂层模具相比，复合金刚石涂层模具的寿命提升近 20 倍。

关键词：微米晶粒；纳米晶粒；复合金刚石薄膜；硬质合金拉拔模具；交替碳源

(Edited by Bing YANG)